Selenourea–Ca 2+ Reactions in Gas Phase. Similarities and Dissimilarities with Urea and Thiourea

ARTICLE *in* THE JOURNAL OF PHYSICAL CHEMISTRY B · JUNE 2008

Impact Factor: 3.3 · DOI: 10.1021/jp711927h · Source: PubMed

Selenourea−Ca^{2+} Reactions in Gas Phase. Similarities and Dissimilarities with Urea and Thiourea

Cristina Trujillo, Otilia Mó, and Manuel Yáñez*

Departamento de Química, C-9. Universidad Autónoma de Madrid. Cantoblanco, 28049-Madrid, Spain

Jeanine Tortajada and Jean-Yves Salpin*

Université d'Evry Val d'Essonne, Laboratoire Analyse et Environnement pour la Biologie et l'Environnement, CNRS UMR 8587, Bâtiment Maupertuis, Boulevard François Mitterrand, 91025 Evry Cedex, France

Received: December 20, 2007; In Final Form: February 1, 2008

The gas-phase reactions between Ca^{2+} and selenourea were investigated by means of electrospray/tandem mass spectrometry techniques. The MS/MS spectra of $[Ca(selenourea)]^{2+}$ complexes show intense peaks at *m*/*z* 43, 121, 124, and 146 and assigned to monocations produced in different coulomb explosion processes. The structures and bonding characteristics of the stationary points of the $[Ca(selenourea)]^{2+}$ potential energy surface (PES) were theoretically studied by DFT calculations carried out at the B3LYP/6-311+G(3df,2p)//B3LYP/6-311+G(d,p) level. The analysis of the topology of this PES allows identification of H_2NCNH^+, $CaSeH^+$, $selenourea^{+\cdot}$ and $CaNCSe^+$ ion peaks at *m*/*z* 43, 121, 124, and 146, respectively. The reactivity of selenourea and the topology of the corresponding potential energy surface mimic that of thiourea. However, significant dissimilarities are found with respect to urea. The dissociative electron-transfer processes, not observed for urea, is one of the dominant fragmentations for selenourea, reflecting its much lower ionization energy. Similarly, the coulomb explosions yielding $CaXH^+ + H_2NCNH^+$ (X = O or Se), which for urea are not observed, are very favorable for selenourea. Finally, while in urea the loss of NH_3 competes with the formation of NH_4^+, for selenourea the latter process is clearly dominant.

Introduction

The alkaline-earth dications are involved in many biological processes.[1−3] For example, it is well-established that they induce proton transfer between guanine and cytosine, regulate muscle contraction, and stabilize interprotein complexes[4] and ribozymes.[5] To get some insight into the mechanisms which, at a molecular level, are responsible for these kinds of processes, we have decided to carry out systematic investigations of reactions between doubly charged metal cations and small model systems, such as formamide, urea, glycine, uracil, and thiouracils, which may be considered as fragments of the more complicated biochemical compounds.[1−8] The combination of mass spectrometry techniques and density functional theory calculations have proved to be a good and reliable approach to get useful information on the way the metal dication−neutral base interactions occur and to provide reaction mechanisms that offer a rationale to the experimental observations.[5,8−24] When dealing with doubly or multiply charged species, the electrospray ionization (ESI) techniques[5−22] are particularly useful, since they allow production of these species in the gas phase, through an energetically mild procedure. We have recently focused our attention on Ca^{2+}, because of its biochemical relevance, and we have already reported the analysis of the unimolecular reactivity of Ca^{2+}−urea[1] and Ca^{2+}−thiourea.[9] These studies showed some similarities between both systems but also significant and interesting dissimilarities. Hence, we have considered it of interest to extend our analysis to the Se-containing analogue, in order to investigate whether its reactivity differs or not from that of the other two compounds, and because selenourea is also very relevant from a biochemical point of view, due to its important antioxidant role[25] and to its behavior as an effective superoxide radical scavenger.[23]

Experimental Section

Electrospray mass spectra were recorded on a QSTAR PULSAR i (Applied Biosystems/MDS Sciex) hybrid instrument (QqTOF) fitted with a nanospray source. Typically, 6 μL of aqueous mixtures of calcium chloride and selenourea (ratio 1:1, 10^{-3} mol L^{-1}) were nanosprayed (20−50 nL/min) using borosilicate emitters (Proxeon). Samples were ionized using an 800 V nanospray needle voltage and the lowest possible nebulizing gas pressure (tens of millibars). The declustering potential (DP, also referred to as "cone voltage" in other devices), defined as the difference in potentials between the orifice plate and the skimmer (grounded), ranged from 0 to 60 V. The operating pressure of curtain gas (N_2) was adjusted to 0.7 bar by means of an electronic board (pressure sensors), as a fraction of the N_2 inlet pressure. To improve ion transmission and subsequently sensitivity during the experiments, collision gas (CAD, N_2) was present at all times for collisional focusing in both the Q0 (ion guide preceding Q1 and located just after the skimmer) and Q2 (collision cell) sectors. For MS/MS spectra, the different complexes of interest were mass selected using quadrupole Q1 and allowed to collide with nitrogen gas at various nominal collision energies ranging from 7 to 17 eV in the laboratory frame (the collision energy is given by the difference between the potentials of Q0 and Q2), with the

* Author to whom correspondence should be addressed. E-mail: manuel.yanez@uam.es; jean-yves.salpin@univ-evry.fr.

10.1021/jp711927h CCC: $40.75
Published on Web 04/05/2008

resulting fragments separated by the time-of-flight (TOF) analyzer after orthogonal injection. Setting the CAD parameter to 1 during MS/MS experiments resulted in pressure values of $1-2 \times 10^{-5}$ Torr as measured by the ion gauge located outside the collision cell. It has been reported[26] that the pressure inside the collision cell is on the order of 10 mTorr. At this pressure and given the dimension of the LINAC collision cell (about 22 cm long), one can find that the mean free path for a N_2 molecule is about 5 mm. So, at this pressure not only N_2 molecules but also complexes of interest (which have higher collision cross-sections) may undergo tens of collisions along their path through Q2. Note that this estimate is a lower limit since N_2 also enters Q0 and Q1 for collisional focusing. Consequently, even with the minimum amount of N_2 inside the collision cell, we are certainly still under a multiple collision regime.

Selenourea and calcium salt were purchased from Aldrich and were used without further purification. All the measurements presented hereafter were carried out in 100% water purified with a Milli-Q water purification system. Unless otherwise noted, throughout this paper the *m*/*z* of any selenium-containing ion will always refer to the one containing the isotope of highest natural abundance (^{80}Se).

Computational Methods. The geometries of neutral selenourea (SeU) as well as those of the different stationary points of the $[Ca(SeU)]^{2+}$ potential energy surface were optimized using the hybrid density functional B3LYP method, which combines Becke's three-parameter nonlocal hybrid exchange potential[27] with the nonlocal correlation functional of Lee, Yang, and Parr.[28] These calculations were performed using the 6-311+G(d,p) basis set for all atoms in the system. The harmonic vibrational frequencies of the different stationary points of the potential energy surface (PES) have been calculated at the same level of theory in order to identify the local minima and the transition states (TS), as well as to estimate the corresponding zero-point energy (ZPE) corrections, which were scaled by the empirical factor 0.985.[29] To assess the connectivity between each transition state and the minima to which it evolves, we have used the intrinsic reaction coordinate (IRC) procedure as implemented in the Gaussian-03 suite of programs.[30]

To obtain more reliable energies for both local minima and transition states, final energies were re-evaluated at the B3LYP/6-311+G(3df,2p)//B3LYP/6-311+G(d,p)+ZPE level. The binding energy was calculated using these final energies, by subtracting from the energy of the most stable $[Ca(SeU)]^{2+}$ complex the energy of selenourea, in its most stable conformation, and the energy of Ca^{2+}, after including the ZPE corrections.

The bonding within the different local minima was analyzed by evaluating the molecular graph of the most stable $[Ca(SeU)]^{2+}$ adducts and by calculating the corresponding energy density contour map within the framework of the atoms in molecules (AIM) theory.[31] For this purpose, we located the relevant bond critical points (BCP) and evaluated the electron density at each of them using the AIMPAC suite of programs.[32] The relative changes in the electron density at the different BCPs offer information in the bonding perturbation undergone by the base upon Ca^{2+} association.[2] On the other hand, the sign of the energy density within each bonding region clearly indicates the covalent or ionic nature of the interaction.[33,34]

Results and Discussion

Mass Spectrometry. A typical nanoelectrospray spectrum obtained at DP = 10 V for a 1:1 aqueous mixture of $CaCl_2$/selenourea is given in Figure 1. Like that for urea[1] and thiourea,[9] abundant hydrated Ca^{2+} ions $[Ca(H_2O)_n]^{2+}$ (n = 1, 2, and 3) are detected at *m*/*z* 28.98, 37.99, and 46.99, respectively. Their intensity quickly decreases as the declustering potential is increased. Calcium hydroxide (*m*/*z* 56.96) is also very intense over the whole range of DP values but is presently not the base peak. The electrospray spectrum is indeed dominated by an ion detected at *m*/*z* 124.94 corresponding to protonated selenourea $(SeU)H^+$. Generally, ions incorporating the selenium atom are easily recognizable due to the characteristic isotopic pattern of this particular element (see inserts in Figure 1). Careful examination of the mass spectrum shows that this particular mass peak in fact corresponds to a mixture of two species, namely the protonated and radical cation of selenourea (*m*/*z* 123.94). This prominent peak remains the base peak regardless of the DP value.

Interaction between selenourea and calcium dication gives rise to both singly and doubly charged complexes. Singly charged complexes of general formula $[Ca(SeU)_nH)]^+$ (n = 1, 2) were quite easy to detect (*m*/*z* 162.88 and 286.82). In contrast, only one doubly charged complex $[Ca(SeU)]^{2+}$ (*m*/*z* 81.95) is observed in weak abundance. Its observation was not straightforward, and optimization of the metal:ligand ratio did not result in any significant improvement of its intensity. In fact, its abundance was found to be particularly sensitive to two interdependent parameters, first the chosen mass range which controls the frequency of the orthogonal injection pulse, and second the way that ions are transferred through the first quadrupole. Despite extensive tuning, the intensity of the complex remained low but sufficient to perform MS/MS experiments. A new selenium-containing ion appears at *m*/*z* 246.90 when the cone voltage is increased. Its isotopic distribution is characteristic of the presence of two selenium atoms, and the mass to charge ratio measured (246.9007) is consistent with the general formula $[C_2,H_7,N_4,Se_2]^+$ whose monoisotopic mass is equal to 246.9001. This general formula formally corresponds to a protonated dimer of selenourea (not observed) that could have lost H_2. In addition, this particular ion is observed neither with urea nor with thiourea and does not come from the $[Ca(SeU)_2\text{-}H)]^+$ complex, as this latter ion species only loses intact selenourea upon collision. A detailed structural characterization of this ion is clearly beyond the scope of the present paper, but complementary experiments are in progress given its specific nature.

MS/MS spectra of the $[Ca(SeU-H)]^+$ and $[Ca(SeU)]^{2+}$ ions were recorded at various collision energies and are illustrated by Figure 2a and 2b, respectively. During this study, the smallest value of the nominal center of mass collision energy in the (E_{cm}) for which sufficient amount of fragment ions can reach the detector, was 2.0 eV, and at this value, dissociation of the doubly charged complex already occurs. The unimolecular reactivity of the singly charged ion upon collision is strictly similar to that observed with urea[1] and thiourea.[9] Two product ions are detected at *m*/*z* 145.88 and 55.98, which correspond to loss of ammonia and [H,N,C,Se], respectively. By contrast, the reactivity of the dication is greatly enhanced. Variations in mass to charge ratios when choosing a different selenium isotope allow both selenium-containing and doubly charged species to be easily identified. Like for the $[Ca(SeU) - H]^+$ ion, elimination of ammonia and [H,N,C,Se] are observed, leading to ions at *m*/*z* 73.45 and 28.49, respectively. Their intensity remains very low, regardless of the collision energy (see Figure 1S of the Supporting Information), whereas eliminations of neutrals were dominant for urea. Bare Ca^{2+} ions (loss of intact selenourea) are also detected but in very weak abundance (less than 1%) and only for E_{cm} values greater than 3.5 eV. All the other

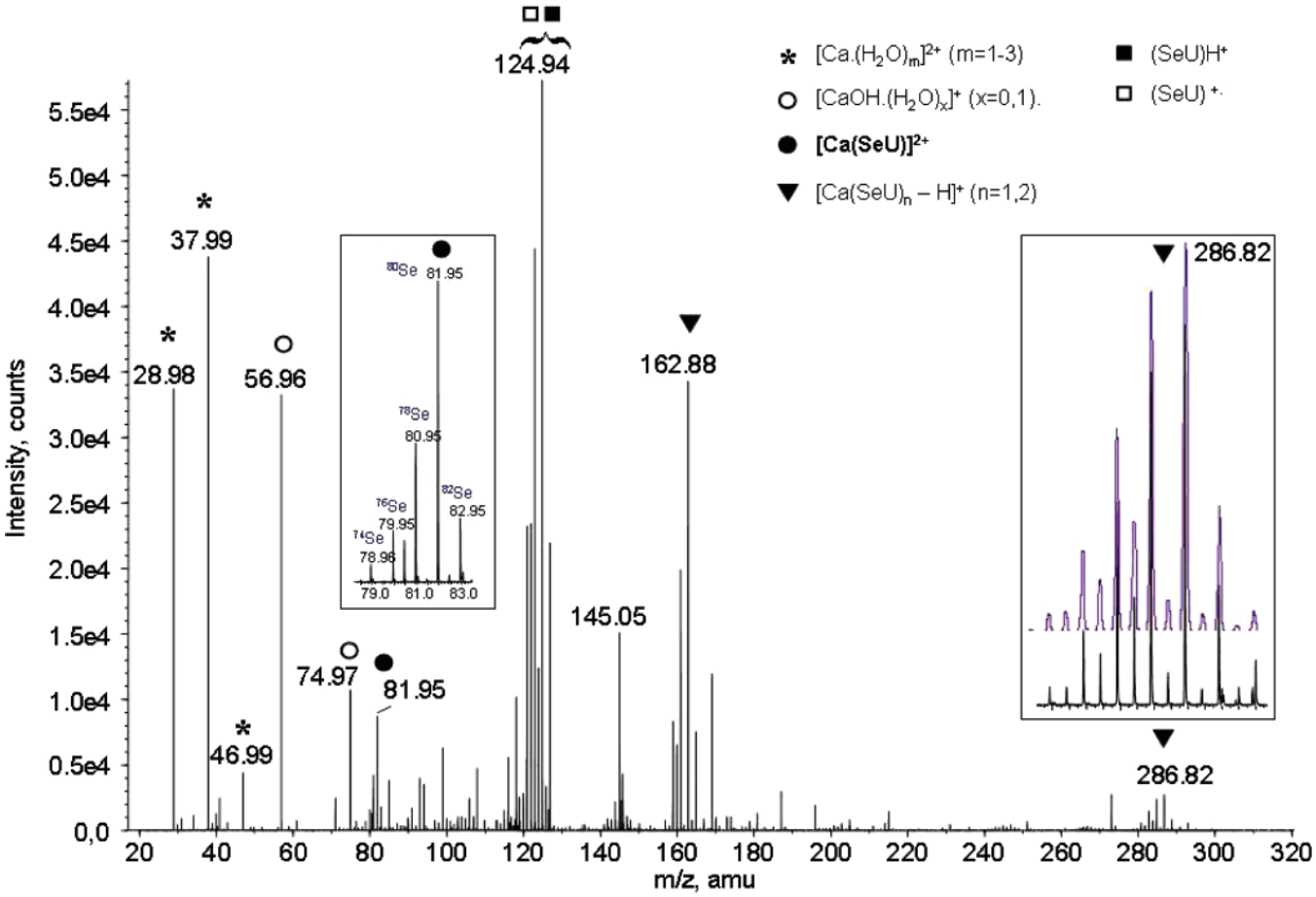

Figure 1. Positive-ion electrospray mass spectrum of an aqueous $CaCl_2$/selenourea (10^{-3} mol L^{-1}/10^{-3} mol L^{-1}) solution.

fragmentation channels may be attributed to coulomb explosion processes. The dissociation pattern of the $[Ca(SeU)]^{2+}$ complex is summarized in Scheme 1.

The major process is the dissociative electron transfer between the ligand and the metallic center, giving rise to Ca^+ (*m*/*z* 39.97) and the radical cation of selenourea (*m*/*z* 123.94). A similar fragmentation has been observed with thiourea but is particularly favored with selenourea because of its lower ionization energy (see discussion below). This electron transfer certainly accounts for the presence of the *m*/*z* 123.94 ion on the electrospray spectrum (Figure 1). Examination of Figure 1S show that the intensity of ionized selenourea regularly increases with the collision energy and then decreased after E_{cm}=3.5 eV. This may be attributed to a secondary fragmentation leading to ions at *m*/*z* 106.92 and *m*/*z* 43.03, as confirmed by the MS/MS spectrum of selenourea radical cation (see Figure 2S of the Supporting Information). Note that formation of *m*/*z* 107 ions from ionized selenourea had been recently reported.[35] Consistently, the intensity of the *m*/*z* 43.03 ion appears particularly important at high collision energies, compared to the situation with thiourea.[9]

Partner peaks arising from the coulomb explosion processes should have in principle the same intensity. However, at moderate collision energy (that is before occurrence of secondary fragmentation processes), and like that for both urea−Ca^{2+} and thiourea−Ca^{2+} systems, the lightest ions (*m*/*z* 18.03, 39.97, 43.03, and 55.98) are systematically less intense than the heaviest ones (*m*/*z* 145.88, 123.94, 120.88, and 107.93, respectively). This effect is particularly pronounced for the three first pairs. Similar findings have been also previously reported for alcohols[36] and acetonitrile.[37] This phenomenon has been interpreted in terms of different radial ion energies, with the lighter ions generated by the coulomb explosion gaining most of the radial energy and therefore having a much higher velocity than the relatively high mass ions. This might lead to unstable ion trajectory within the instrument and account for smaller abundance for the lightest species. This effect may be even more pronounced in our QqTOF instrument, because of low-mass discrimination during the orthogonal injection step.

Structures and Relative Stabilities of $[Ca(SeU)]^{2+}$ Adducts. The geometries of the three lowest-energy structures of the $[Ca(SeU)]^{2+}$ adducts are given in Figure 3. For these three structures, the bonding scheme is similar to those observed with urea[1] and thiourea,[9] and the same energy order is found. The global minimum **1** is a monodentate complex in which the metal dication is attached to the selenium atom. Like that for thiourea, Ca^{2+} is located in the plane that bisects the NCN angle of the base and forms an angle of 113.8° with the C═Se bond, while for urea the metal dication lies in the same plane of the molecule. The preference for a bent structure for the seleno derivative is related to the size of the selenium lone pairs. In the carbonyl group (urea), both lone pairs are small and the cation locates between both to enhance polarization effects. Conversely, the lone pairs of selenium are much larger and the specific interaction with a single lone pair is clearly favored.

A second local minimum, **2**, is found only 8.4 kJ mol^{-1} above **1**. In this case, the metal bridges the atom of selenium and one of the amino groups. The third adduct, **3**, in which the dication bridges both amino groups, appears significantly higher in energy (140.6 kJ mol^{-1}) with respect to the global minimum. The selenourea−Ca^{2+} binding energy (415.4 kJ mol^{-1}) was calculated to be slightly greater than that of thiourea (404.0 kJ

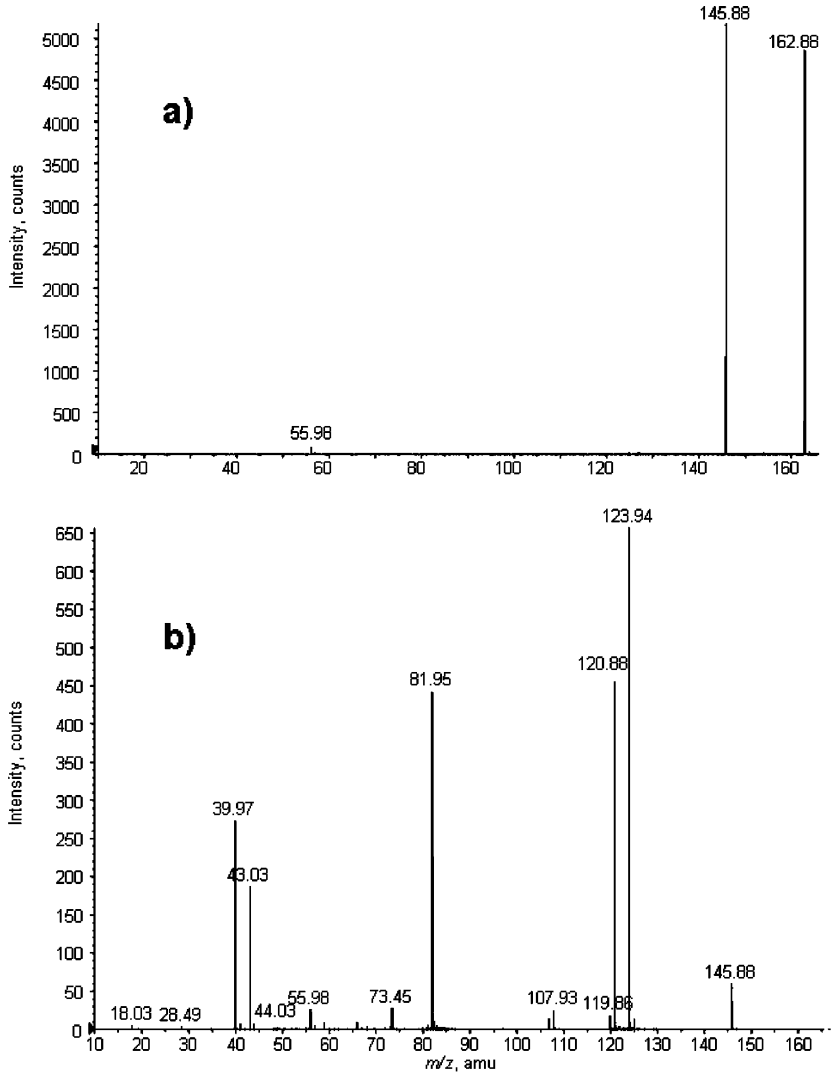

Figure 2. Low-energy CID spectra of (a) $[Ca(SeU-H)]^+$ and (b) $[Ca(SeU)]^{2+}$ complexes recorded at DP = 35 V and E_{cm} = 2.4 and 3.5 eV, respectively.

SCHEME 1

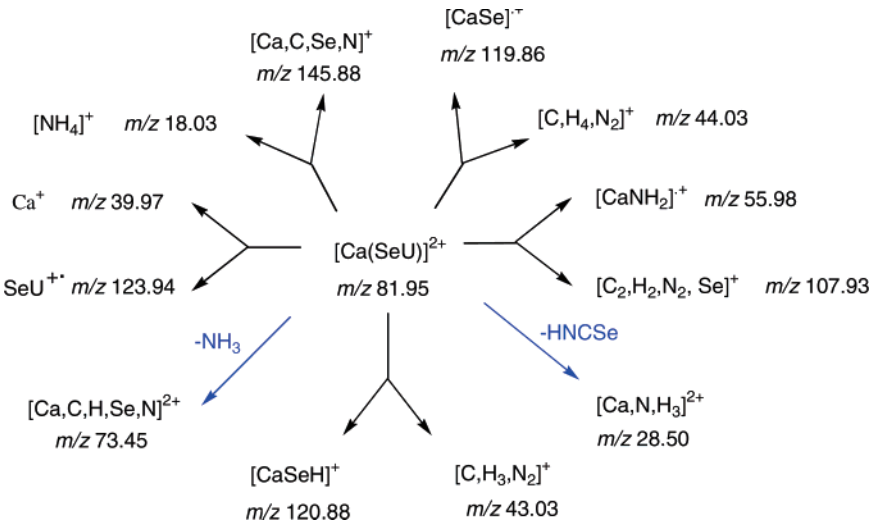

mol^{-1})[9] but slightly smaller than that for urea$-Ca^{2+}$ (453.0 kJ mol^{-1}),[1] indicating the preference of Ca^{2+} for oxygen.

A topological analysis of the electron density of these three minima, as compared to isolated selenourea, reveals that the selenourea$-Ca^{2+}$ interaction is essentially electrostatic. This is clearly established by the positive value of the energy density in the region between both subunits (see Figure 4). However, strong polarization effects, caused by the metal dication, which are the origin of significant bond perturbations, are also evident and similar to those discussed in ref 9 for thiourea. We will

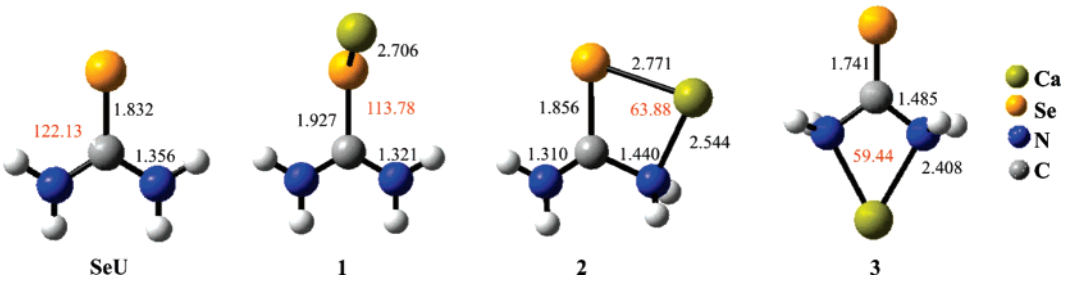

Figure 3. Optimized geometries for the most stable selenourea−Ca^{2+} adducts. Bond lengths are in angstroms and bond angles in degrees. For the sake of comparison we have also included the optimized geometry of the isolated selenourea.

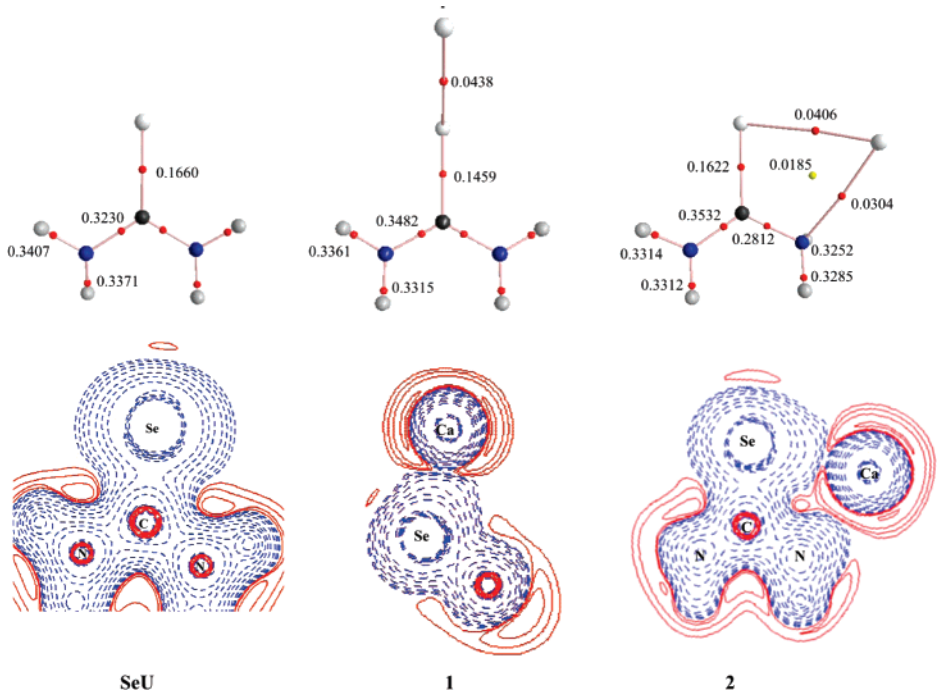

Figure 4. Molecular graphs and contour maps of the energy density for the two most stable [Ca-selenourea]$^{2+}$ complexes. In the plot of the energy density, blue dashed lines correspond to negative values of $H(\mathbf{r})$ and solid red lines to positive values. In the molecular graphs both the BCPs (red dots) and the ring critical points (yellow dots) are shown. Electron densities are in atomic units (a.u.).

summarize the most important ones. Bonding of Ca^{2+} to Se in complex **1** leads to a decrease in the electron density at the C═Se bond (see Figure 4), which accordingly lengthens 0.095 Å, while its stretching frequency appears 23 cm^{-1} red-shifted. The polarization of the electron density toward the metal triggers a much better conjugation of the amino lone-pairs, which is reflected in the complete planarity of both groups in the complex and in the increase of the electron density at the C−N BCP. Consistently, the CN bonds shorten and the stretching frequencies, which are coupled as symmetric and antisymmetric combinations, are blue-shifted by 52 and 39 cm^{-1}, respectively. In complex **2**, where the metal interacts only with one amino group, this symmetry is broken, and the CN stretching frequencies are decoupled. The topology of the electron density reveals that the C−N bond directly interacting with the metal is also strongly activated (it lengthens 0.084 Å) while the noninteracting C−N bond is reinforced and shortens by 0.046 Å. As expected, the effects on the C═Se bond are smaller than in complex **1** (see Figure 4), this bond lengthens only 0.024 Å, and its stretching frequency is red-shifted by 14 cm^{-1}.

Unimolecular Reactivity of the$[Ca(SeU)]^{2+}$ Complexes. The potential energy surface associated with the $[Ca(SeU)]^{2+}$ system is quite complex as is the observed unimolecular reactivity, so for the sake of clarity, we will present this surface split into two energy profiles. In Figure 5 we have considered all the reaction pathways leading to the following products: Ca^+ + selenourea$^{+\cdot}$, $CaNH_2^+$ + [N, H_2, C, Se]$^+$, $CaSeH^+$ + NH_2-CNH^+, SeH_2^+ + NH_2CNCa^+. Figure 6 contains the reaction pathways associated with the loss of neutrals (namely NH_3 and HNCSe) and with coulomb explosions yielding NH_4^+ cations. The total energies of the different stationary points as well as the corresponding ZPE are summarized in Table S1 of the Supporting Information.

In both Figures 5 and 6 we have distinguished the mechanisms associated with the loss of a neutral fragment (black solid lines) from those corresponding to coulomb explosions (red dashed lines), in which two monocations are formed.

Reaction Mechanisms Associated with the Energy Profiles in Figure 5. The most favorable process of this energy profile is the isomerization of the global minimum **1** to complex **2**, by means of an internal rotation of the CaSe moiety, and associated with an energy barrier on only 17.8 kJ mol^{-1}, but the mechanisms with an origin in adduct **2** will be discussed separately. Apart from the **1**→**2** process, three other reaction paths may be envisaged with an origin in the global minimum. One of them is the dissociative electron-transfer process which yields Ca^+ + selenourea$^{+\cdot}$. The second possible reaction path corresponds to the **1**→**3** isomerization through a symmetrical

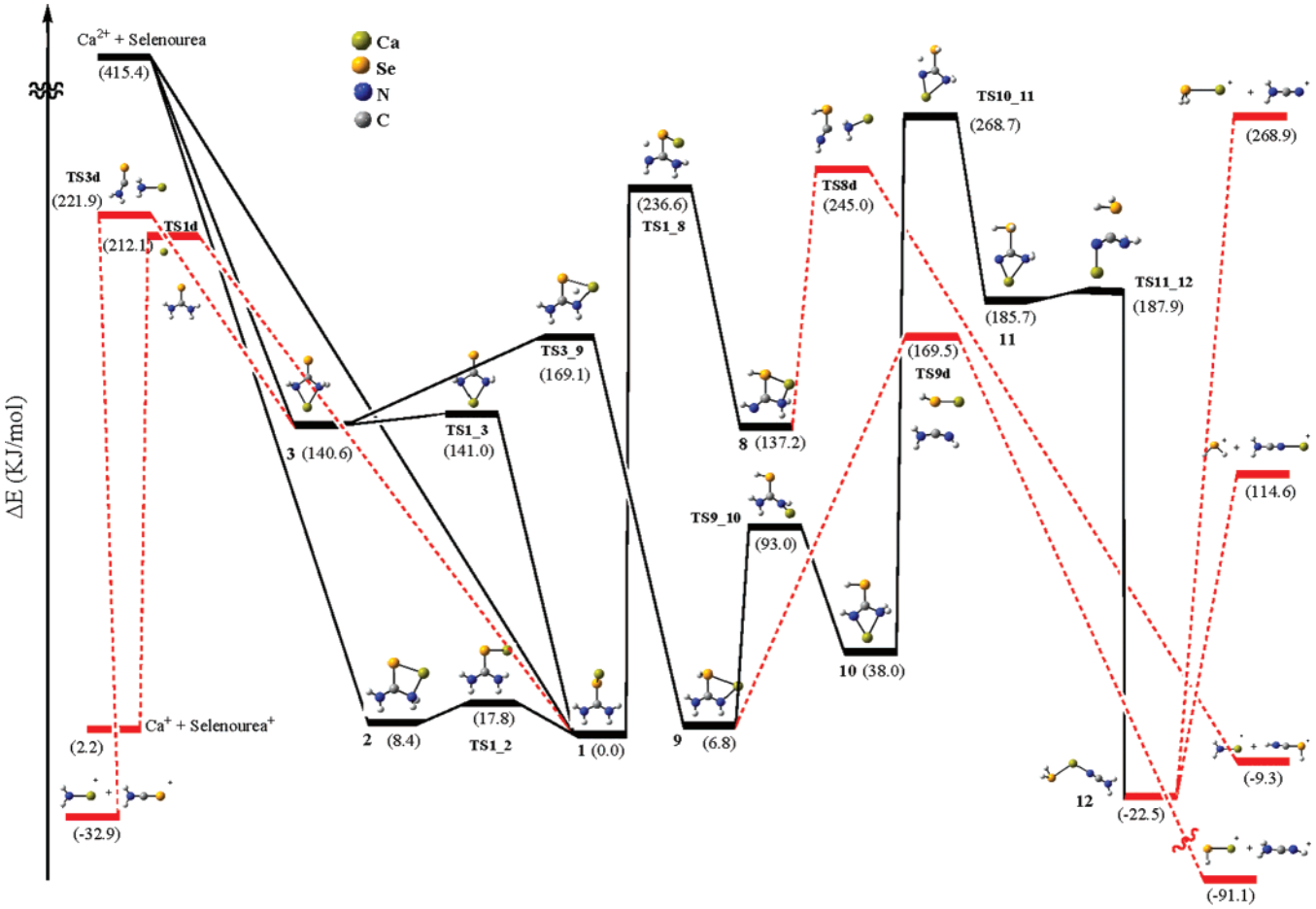

Figure 5. Energy profiles associated with the reaction pathways leading to the following products: Ca^+ + selenourea$^{+\cdot}$, $CaNH_2^+$ + [N, H_2, C, Se]$^+$, $CaSeH^+$ + NH_2CNH^+, SeH_2^+ + NH_2CNCa^+. Dashed red lines correspond to mechanisms associated with coulomb explosions.

displacement of the Ca to lie in the plane of amino groups. The third process corresponds to a 1,3-H shift from the amino group to the selenium atom yielding minimum **8**. Three different reaction paths have their origin in **3**. One corresponds to a coulomb explosion that splits this complex into two charged fragments H_2NCa^+ + H_2NCSe^+, which might correspond to the ions detected at *m*/*z* 55.98 and *m*/*z* 107.93, respectively. These two ions can also be produced through a coulomb explosion of **8**, but in this case one of hydrogens of the amino group is bonded to the metal dication, giving rise to the $HNCSeH^+$ moiety. Not only is this latter process less favorable thermodynamically, but it is also characterized by a higher energy barrier. Hence, we can conclude that the *m*/*z* 107.93 peak should preferentially correspond to H_2NCSe^+ species.

Adduct **3** may also evolve toward minimum **9**, in which the metal bridges a SeH group and an imino group. Once **9** is formed, it can undergo a coulomb explosion, giving rise to the ionic products $CaSeH^+$ (*m*/*z* 120.88) + H_2NCNH^+ (*m*/*z* 43.03). This dissociation route is one of the most favorable in this energy profile, in agreement with the high intensity of the corresponding peaks onto the MS/MS spectrum (Figure 2). Alternatively, structure **9**, through two intermediates **10** and **11**, yields the very stable complex **12**, which lies 22.5 kJ mol^{-1} below the global minimum **1**. This minimum may subsequently evolve according to two product channels, namely SeH_2^+ + H_2NCNCa^+ and H_2SeCa^+ + H_2NCN^+. None of these four ions are observed experimentally. This might be attributed to the very high energetic barrier separating adducts **10** and **11**. In addition both processes are very endothermic with respect to minimum **12**.

Reaction Mechanisms Associated with the Energy Profiles in Figure 6. Minima **2** and **3** can be obtained either from direct attachment of the metal dication to selenourea or, as we have mentioned in the previous section, by isomerization of the global minimum **1**.

The most favorable process starting from **2** is the isomerization, giving rise to the adduct **3**, through an internal rotation of the $CaNH_2$ group. The second most favorable process corresponds to a coulomb explosion leading to $CaNH_2^+$ + $SeCNH_2^+$, which, as discussed above, can also originate in adduct **3**. A comparison of Figures 5 and 6 indicates that both coulomb explosions are equally favorable.

The third process involving structure **2** is the formation of minimum **4** by means of one 1,3-H shift between the two amino groups. However, the lowest energy pathway to reach this intermediate is through structure **9**. As discussed above (see Figure 5), the activation barrier connecting **3** and **9** is 169 kJ mol^{-1}, and that connecting **9** and **4** (see Figure 6) is only slightly higher (179.4 kJ mol^{-1}) but both of them significantly lower than that connecting **2** and **4** (250.3 kJ mol^{-1}).

From the intermediate **4**, several reaction paths may be considered. The least energy demanding is the formation of the minimum **6** through **TS4_6**, in which NH_4^+ ion interacts with the $NCSeCa^+$ moiety. This adduct gives rise to the two most thermodynamically favorable product channels of the global potential energy surface, which yield NH_4^+ and [Ca,N,C,Se]$^+$ (this may account for peaks detected at *m*/*z* 18.03 and 145.88, respectively on the MS/MS spectrum). In the more exothermic one (−196.6 kJ mol^{-1}), Ca interacts with the three atoms of

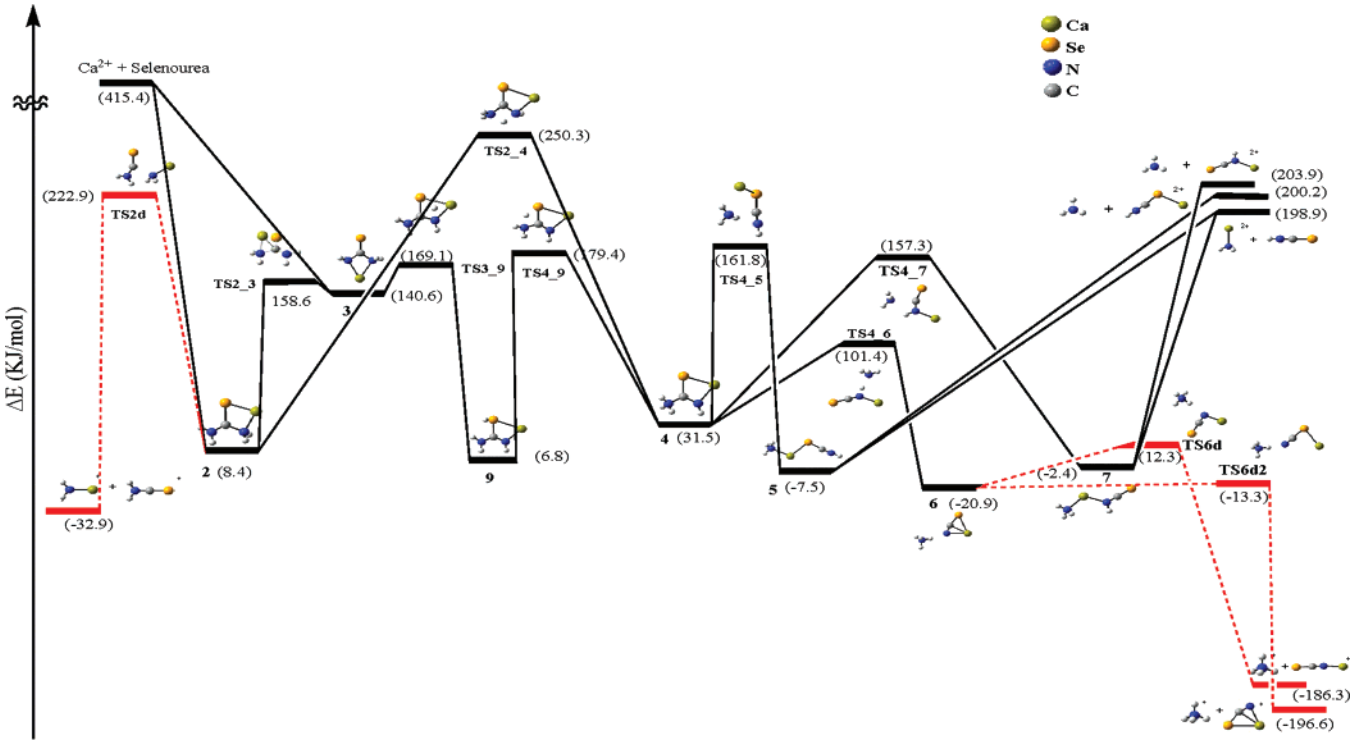

Figure 6. Energy profiles associated with the reaction pathways corresponding the loss of neutrals (namely NH_3 and HNCSe) and with coulomb explosions yielding NH_4^+ cations. Dashed red lines correspond to mechanisms associated with coulomb explosions.

the NCSe moiety, while in the less exothermic one (−186.3 kJ mol^{-1}) the metal is solely linked to the selenium atom.

The mechanisms for the loss of neutral molecules, NH_3 and HNCSe, also have their origin in minimum **4**, either directly (not shown in the figure) or through the formation of the two very stable intermediates **5** and **7**. The difference between these two minima is the connectivity of the Ca atom. In the former (adduct **5** $[NH_3\cdots Ca\cdots SeCNH]^{2+}$) the metal dication is linked to the selenium atom, while in adduct **7** ($[NH_3\cdots Ca\cdots N(H)CSe]^{2+}$) it is bonded to the nitrogen atom. Both complexes may lead to the fragments $[Ca-NH_3]^{2+}$ + H−N═C═Se or, through the complementary dissociation channels, to elimination of ammonia and formation of either $[Ca\cdots SeCNH]^{2+}$ (adduct **5**) or $[Ca\cdots N(H)CSe]^{2+}$ (adduct **7**). Our data show that compared to the coulomb explosion processes, these three mechanisms are not thermodynamically favorable, which is consistent with the very low abundance of the corresponding ions on the MS/MS spectrum (*m*/*z* 28.49 and 73.45). Our calculations also suggest that the Ca^{2+} affinity of ammonia and HNCSe are roughly comparable. So, the lower abundance of the *m*/*z* 29.49 ions compared to *m*/*z* 73.45 might be due to low mass discrimination within the instrument. Finally, our data also suggest that the basicity toward Ca^{2+} of the nitrogen and selenium center of the selenoisocyanic acid is comparable.

A Comparison between the Systems: Urea-Ca^{2+}, Thiourea−Ca^{2+}, and Selenourea−Ca^{2+}. Based on our previous studies, a comparison of the unimolecular reactivity of the three systems $[Ca(U)]^{2+}$, $[Ca(TU)]^{2+}$, and $[Ca(SeU)]^{2+}$ can be made. In the present study, MS/MS spectra were recorded at a collision energy ranging from 7 to 17 eV in the laboratory frame. This corresponds to center-of-mass collision energies starting from 2.04 eV. At the lowest collision energy, only the ions arising from coulomb explosions are detected. But globally, the reactivity of selenourea mimics that of thiourea, which, in turn, as reported previously[9] differs sensibly from that of urea. One of the most important dissimilarities between urea and its S- and Se-containing analogues arises from the large difference between the corresponding ionization energies, which for urea (10.27 eV[38]) is sizably larger than for thiourea (8.50 eV[38]) and for selenourea (7.80 eV, as estimated at the B3LYP/6-311+G-(3df,2p)//B3LYP/6-311+G(d,p) level). Accordingly, one can see that the formation of the radical cation of the ligand is a more and more facile process, on going from urea to thiourea and to selenourea, as attested by the increasing abundance of this species at a given collision energy. Bear in mind that this peak was not observed for urea.

In the case of the $[Ca(TU)]^{2+}$ and $[Ca(SeU)]^{2+}$ systems, losses of neutral molecules are very minor processes. Loss of NH_3 requires much more energy than the proton transfer leading to the NH_4^+ moiety. This is a difference with respect to the $[Ca(U)]^{2+}$ unimolecular reactivity, where the energy requirements to form NH_4^+ or to lose NH_3 are rather similar. Consistently, formation of doubly charged fragments is much more important for urea. Also we can say that in the three cases the loss of NH_4^+ system is the thermodynamically most favorable reaction overall.

Another important difference between these three systems concerns the coulomb explosions giving rise to $CaXH^+ + H_2NCNH^+$ (X = S or Se). While these processes are among the most favorable for thiourea and selenourea, it is not observed in Ca^{2+}-urea reactions. This is a consequence of the substantial difference between the barriers associated with the hydrogen shifts from the amino groups toward the carbonyl (thiocarbonyl, selenocarbonyl) group. While in selenourea and thiourea these hydrogen shifts involve activation barriers rather similar to those of the different coulomb explosions and to those of the hydrogen shifts between the amino groups, in urea these barriers are much higher in energy, and therefore the associated processes very unfavorable. This difference just reflects the fact that both enethiols and selenols are intrinsically more stable than enols with respect to the corresponding keto forms.[39,40] On the other hand, the energy gap between the keto and enol forms decreases

upon Ca^{2+} interaction by 58 kJ mol^{-1} for selenourea, while it increases by 11 kJ mol^{-1} for urea. The consequence of these differences is that the H-shift processes from the amino group toward the C = X (X = O, S, Se) group, that in urea are very unfavorable, in selenourea and thiourea become energetically accessible, requiring activation energies similar to those involved in H-shifts between the amino groups.

Conclusions

This study showed that the unimolecular reactivity of selenourea−Ca^{2+} bears a great similarity with the reactivity of the thiourea−Ca^{2+} system, obtaining for both cases very similar potential energy surfaces. The most remarkable differences between selenourea and urea are a consequence of the low ionization energy of former with respect to latter, the enhanced relative stability of selenols with respect to enols, and to the fact that while selenols are significantly stabilized by Ca^{2+} association with respect to the keto forms, enols are slightly destabilized. The consequence of the first difference is that the dissociative electron-transfer process, not observed for urea, is one of the dominant fragmentations for selenourea. The second difference is reflected in the fact that $CaXH^+ + H_2NCNH^+$ (X = O or Se) coulomb explosions, which for urea are not observed, become very favorable for selenourea. The third significant difference is that while in urea the loss of neutral fragments such as NH_3 compete with alternative coulomb explosions yielding NH_4^+, for selenourea NH_3 is produced in very low abundance.

Acknowledgment. This work has been partially supported by the DGI Project No. BQU2003-00894, by the COST Action D26/0014/03, and by the Project MADRISOLAR, ref: S-0505/PPQ/0225 of the Comunidad Autónoma de Madrid. A generous allocation of computing time at the CCC of the UAM is also acknowledged.

Supporting Information Available: Intensity of product ions generated upon CID of $[Ca(SeU)]^{2+}$ ions; MS/MS spectrum of the radical cation of ^{80}Se-selenourea generated under electrospray conditions; total energies of the stationary points of the $[Ca(SeU)]^{2+}$ potential energy surface and complete reference 29. This material is available free of charge via the Internet at http://pubs.acs.org

References and Notes

(1) Corral, I.; Mó, O.; Yáñez, M.; Salpin, J.-Y.; Tortajada, J.; Radom, L. *J. Phys. Chem. A* **2004**, *108*, 10080.

(2) Corral, I.; Mó, O.; Yáñez, M. Bonding and Bonding Perturbation in Ion-Molecule Interactions in the Gas Phase. In *Encyclopedia of Computational Chemistry*; URL: http/www.mrw.interscience.wiley.com/eccarticles/cn0062/frame.html, 2004.

(3) Lamsabhi, A. M.; Mó, O.; Yáñez, M.; Alcamí, M.; Tortajada, J. *ChemPhysChem* **2004**, *5*, 1.

(4) Palacios, A.; Corral, I.; Mó, O.; Martín, F.; Yáñez, M. *J. Chem. Phys.* **2005**, *123*, 014315 (1.

(5) Guillaumont, S.; Tortajada, J.; Salpin, J.-Y.; Lamsabhi, A. M. *Int. J. Mass Spectrom.* **2005**, *243*, 279.

(6) Corral, I.; Mó, O.; Yáñez, M.; Salpin, J.-Y.; Tortajada, J.; Moran, D.; Radom, L. *Chem. Eur. J* **2006**, *12*, 6787.

(7) Lamsabhi, A. M.; Alcamí, M.; Mó, O.; Yáñez, M.; Tortajada, J. *J. Phys. Chem. A* **2006**, *110*, 1943.

(8) Lamsabhi, A. M.; Alcamí, M.; Mó, O.; Yáñez, M.; Tortajada, J.; Salpin, J.-Y. *ChemPhysChem* **2007**, *8*, 181.

(9) Trujillo, C.; Mó, O.; Yáñez, M.; Salpin, J.-Y.; Tortajada, J. *ChemPhysChem* **2007**, *8*, 1330.

(10) Peschke, M.; Blades, A. T.; Kebarle, P. *J. Am. Chem. Soc.* **2000**, *122*, 10440.

(11) Schwarz, H.; Schröder, D. *Pure Appl. Chem.* **2000**, *72*, 2319.

(12) Salpin, J.-Y.; Boutreau, L.; Haldys, V.; Tortajada, J. *Eur. J. Mass Spectrom.* **2001**, *7*, 321.

(13) Salpin, J.-Y.; Tortajada, J. *J. Phys. Chem. A* **2003**, *107*, 2943.

(14) Schröder, D.; Schwarz, H.; Wu, J.; Wesdemiotis, C. *Chem. Phys. Lett.* **2001**, *343*, 258.

(15) Rogalewicz, F.; Louazel, G.; Hoppilliard, Y.; Ohanessian, G. *Int. J. Mass Spectrom.* **2003**, *228*, 779.

(16) Cox, H.; Stace, A. J. *J. Am. Chem. Soc.* **2004**, *126*, 3939.

(17) Belcastro, M.; Marino, T.; Russo, N.; Toscano, M. *J. Mass Spectrom.* **2005**, *40*, 300.

(18) Lee, J. K. *Int. J. Mass Spectrom.* **2005**, *240*, 261.

(19) Rondeau, D.; Rogalewicz, F.; Ohanessian, G.; Levillain, E.; Odobel, F.; Richomme, P. *J. Mass Spectrom.* **2005**, *40*, 628.

(20) Fung, Y. M. E.; Liu, H. C.; Chan, T. W. D. *J. Am. Soc. Mass Spectrom.* **2006**, *17*, 757.

(21) Polfer, N. C.; Oomens, J.; Moore, D. T.; von Helden, G.; Meijer, G.; Dunbar, R. C. *J. Am. Chem. Soc.* **2006**, *128*, 517.

(22) Carl, D. R.; Moision, R. M.; Armentrout, P. B. *Int. J. Mass Spectrom.* **2007**, *265*, 308.

(23) Shi, T. J.; Hopkinson, A. C.; Siu, K. W. M. *Chem. Eur. J.* **2007**, *13*, 1142.

(24) Rimola, A.; Rodriguez-Santiago, L.; Ugliengo, P.; Sodupe, M. *J. Phys. Chem. B* **2007**, *111*, 5740.

(25) Tapiero, H.; Townsend, D. M.; Tew, K. D. *Biomed. Pharmacother.* **2003**, *57*, 134.

(26) Chernushevich, I. V.; Loboda, A. V.; Thomson, B. A. *J. Mass Spectrom.* **2001**, *36*, 849.

(27) Becke, A. D. *J. Chem. Phys.* **1993**, *98*, 1372.

(28) Lee, C.; Yang, W.; Parr, R. *Phys. Rev. B: Condens. Matter* **1988**, *37*, 785.

(29) Scott, A. P.; Radom, L. *J. Phys. Chem.* **1996**, *100*, 16502.

(30) Frisch, M. J. et al. Gaussian03; Revision C.02 ed.; Gaussian, Inc.: Wallingford CT, 2003.

(31) Bader, R. F. W. *Atoms in Molecules. A Quantum Theory*; Clarendon Press: Oxford, 1990.

(32) Bader, R. F. W.; Cheeseman, J. R. AIMPAC, 2000.

(33) Cremer, D.; Kraka, E. *Angew. Chem., Int. Ed. Engl.* **1984**, *23*, 627.

(34) Alcamí, M.; Mó, O.; Yáñez, M.; Cooper, I. L. *J. Phys. Chem. A* **1999**, *103*, 2793.

(35) Gerbaux, P.; Dechamps, N.; Flammang, R.; Reddy, P. N.; Srinivas, R. *Rapid Commun. Mass Spectrom.* **2006**, *20*, 151.

(36) Kohno, J.; Mafune, F.; Kondow, T. *J. Phys. Chem. A* **1999**, *103*, 1518.

(37) Kohler, M.; Leary, J. A. *Int. J. Mass Spectrom. Ion Processes* **1997**, *162*, 17.

(38) *NIST Chemistry Webbook*; Standard Reference Database 69, 1998.

(39) Gonzalez, L.; Mó, O.; Yáñez, M. *J. Phys. Chem. A* **1997**, *101*, 9710.

(40) Sanz, P.; Yanez, M.; Mó, O. *J. Phys. Chem. A* **2002**, *106*, 4661.